1 # Potential Impacts of Future Climate Change and Emission on the

2 # Fate and Transport of PFOS in the Bohai Rim, China

3 Chao Su [a, b], Shuai Song [a], Yonglong Lu [a]*, Baninla Yvette [a, b], Shijie Liu [a], John P. Giesy[c],

4 Deliang Chen[d], Alan Jenkins[e], Andrew Sweetman[e,f]

5

6 [a] State Key Laboratory of Urban and Regional Ecology, Research Center for Eco-Environmental

7 Sciences, Chinese Academy of Sciences, Beijing 100085, China

8 [b] University of Chinese Academy of Sciences, Beijing 100049, China

9 [c] Toxicology Centre and Department of Veterinary Biomedical Sciences, University of

10 Saskatchewan, Saskatoon, Saskatchewan, Canada

11 [d] Department of Earth Sciences, University of Gothenburg, 405 30 Gothenburg, Sweden

12 [e] Centre for Ecology & Hydrology, Wallingford, OX 10 8BB, UK

13 [f] Lancaster Environment Centre, Lancaster University, Lancaster LA1 4YQ, UK

14

15 Corresponding author:

16 *Yonglong Lu

17 Tel: 86-10-62915537

18 Fax: 86-10-62918177

19 E-mail: yllu@rcees.ac.cn

20

21 **Abstract:**

22 Both climate change and contaminant emission rate are expected to affect the transport and fate of

23 POPs. However, studies on their integrative impacts are fewer. This study, taking Perfluorooctane

24 Sulfonate (PFOS) as an example, explored how future climate change and contaminant emission

25 affect the fate of POPs synthetically, as well as urbanization rate being taken into account, using

26 BETR-Urban-Rural (BETR-UR) model, an improved BETR model. The results suggested that

27 climate change had significant effects on the fate of PFOS, with precipitation and temperature

28 being predominant factors, by the following aspects: advection processes, degradation rate, and

29 intermedia transfer processes. Under the "business-as-usual" emission scenario, for most grids, a

30 remarkable decline in PFOS concentration was observed in fresh water and urban soil in the future,

31 particularly in the late 21st century, while coastal water and rural soil displayed an opposite

32 changing trend. Besides, under the integrative effects of reducing emission and climate change

33 scenarios, PFOS concentrations in each compartment decreased sharply over time. Additionally,

34 we discussed the influences of climate change on the fluxes of PFOS to the Bohai Sea. Total sum

35 of emissions increased by 1.61%, 11.80%, 17.04% with increasing precipitation, and sinks by

36 2.59%, 14.30%, 22.24% due to volatilization and degradation flux in 2035, 2065, and 2100,

37 respectively. However, the sum of the emissions was always more than the sum of the sinks in

38 Bohai Sea. The coastal or marine ecosystem should be given greater consideration in the future.

39 This suggests that future assessment of climate change impacts on POPs fate should take emission

40 reduction into consideration.

41 **Keywords:** climate change, emission rate, urbanization, PFOS fate, multimedia model, regional

42 scale

43 1. Introduction

44   Persistent organic pollutants (POPs) are a kind of pollutants with the following properties:

45 persistence, toxicity, and long-range atmospheric transport (LRAT). Due to these properties,

46 particularly the LRAT resulting in dispersed contamination far from source regions, the fate and

47 behavior of POPs have captivated increasing concern from international environmental

48 organizations, governments, academics, and the public. Many researches showed that the fate and

49 behavior of POPs have been affected by various factors, e.g. emission rate, environmental

50 parameters such as temperature, rain rate, and soil solids organic carbon fraction. (Prevedouros et

51 al., 2004a; Prevedouros et al., 2004b). Climate change is having far-reaching effects on the

52 environment and then on the fate of POPs, not only impacted by and impacting on natural

53 processes within the climate system itself, but also anthropogenic activities (e.g., increased

54 emissions of greenhouse gases) (Paul et al., 2012). Direct changes such as temperature rise, and

55 those driven by it (ocean temperature rise, sea-level rise), altered precipitation patterns, wind and

56   ocean current patterns, hence resulted in those indirect changes such as land cover changes.

57   In general, the influencing mechanism of climate change on the environmental behavior and

58   fate of POPs could be described from three aspects. Firstly, it is likely to influence the

59   environmental behavior of POPs by enhancing the volatilization from primary and secondary

60   sources, by influencing their partitioning between soil, sediment, water, and atmosphere, including

61   air-surface exchange, wet/dry deposition, and reaction rates (Teran et al., 2012). Secondly, it could

62   change the solubility of chemicals, and consequently change their concentration and activity in the

63   environment. Then, it could affect the decomposition rate of POPs in the environment (Zhou and

64   Ma, 2013). However, our understanding of these mechanism is mostly qualitative, and a more

65   quantitative description of potential effects is needed (Woehrnschimmel et al., 2013). Recently, a

66   few studies have explored the effects using models under climate change scenarios quantitatively

67   (Gouin et al., 2013; Lamon et al., 2009; Ma and Cao, 2010; Paul et al., 2012). Lamon et al. studied

68   fate and transport of PCBs under a realistic climate change scenario using global multimedia

69   model under steady state (Lamon et al., 2009). On regional scale, Paul et al. and Henry et al.

70   explored the potential implications of future climate and land-cover changes for the fate and

71   distribution of POPs in Europe and Arctic, respectively (Paul et al., 2012; Woehrnschimmel et al.,

72   2013). The common modeled results showed that the effect of climate change on environmental

73   concentrations of POPs was typically up to factors between 1.5 and 2.5 even up to 4 in modeled

74   concentrations. While, PCB 153 displayed a change with the most reduction in burden of up to 40%

75   in some Mediterranean compartments in Europe (Paul et al., 2012). However, the researches

76   combining climate change and emission rate to study the integrated effects are fewer.

77   The objective of this study is to explore how climate change (temperature, precipitation, wind

78   speed, soil carbon stock, and sea-level rise) and emission rate affect the fate of perfluorooctane

79   sulfonate (PFOS), as well as the urban-rural disparities, with a facus on Bohai Rim in China. In

80   this study, the Berkeley-Trent-Urban-Rural (BETR-UR) model was used to run the simulations

81   under the three climate change scenarios (B1, A1B, and A2) in IPCC 2007 and four emission

82   scenarios for three 20-year periods throughout the 21st century (2016-2035, 2046-2065, and

83   2081-2100), relative to the baseline simulation of 2010. Then, it explored the key affecting factors

84   of PFOS, and analyzed the alterations of mass fluxes of PFOS to the Bohai Sea under climate

85   change. This research could provide powerful theoretical support for PFOS emission reduction

86   and ecosystem protection.

87   2.   Methods and Materials

88   2.1 Model description and study area

89   Within the original BETR model based on fugacity concept (Mackay, 2001), a connected

90   system of nine discrete and homogeneous compartments is considered as one segmentation (or

91   grid). BETR model has been successfully applied to model the multimedia fate of chemicals,

92   including the North America (MacLeod et al., 2001; Woodfine et al., 2001), Europe (Prevedouros

93   et al., 2004a; Prevedouros et al., 2004b), and the global environment (MacLeod et al., 2005). The

94   BETR-UR model is an improved BETR model (Song et al, 2016). It takes the effects of

95   urbanization into account, dividing the soil and lower air compartments into urban soil and rural

96   soil, lower urban air and lower rural air, respectively. The urban areas mainly indicated those areas

97   with high population density, including industrial land, built-up land, commercial districts, urban

98   residential areas, municipal land for public facilities, and their buffers. Except for urban areas, we

99   defined rural areas as a combination of rural villages, agricultural land, grassland, forest land, rural

100   residential areas, unused land and so on (Wang et al., 2010). The framework of BETR-UR model

101   is illustrated in Fig. 1. In the BETR-UR model, the environment within each segment contains

102   nine compartments. Specific environmental parameters for an urban area like urban perimeter,

103   urban-rural atmospheric mixing rate, freshwater area of urban area etc. and transfer processes

104   between urban and rural area were also improved. More materials could be found in (Song et al.,

105   2016).
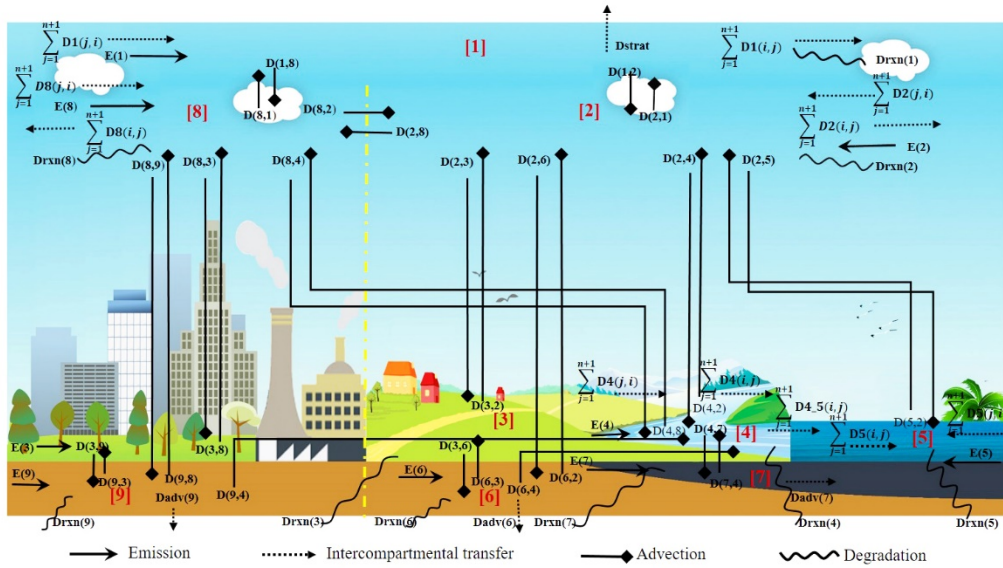
Fig. 1 Contaminant transportation processes in the region *i* linked with *j* in the BETR-UR model.

The Bohai Rim, including part of Bohai Sea and its surrounding area, is one of the most prosperous regions in China. In this paper, the study area included Beijing, Tianjin, Liaoning, Hebei and Shandong provinces and municipalities. A wide range of industries are distributed in this region, including textile treatment, metal plating, production of firefighting chemicals and semiconductor industries, some of which are associated with industrial sources of PFOS and related substances in China (Xie et al., 2013b). Rapid urbanization and industrial development have caused great increase in energy consumption and pollutants emission, further leading to multiple environmental problems.
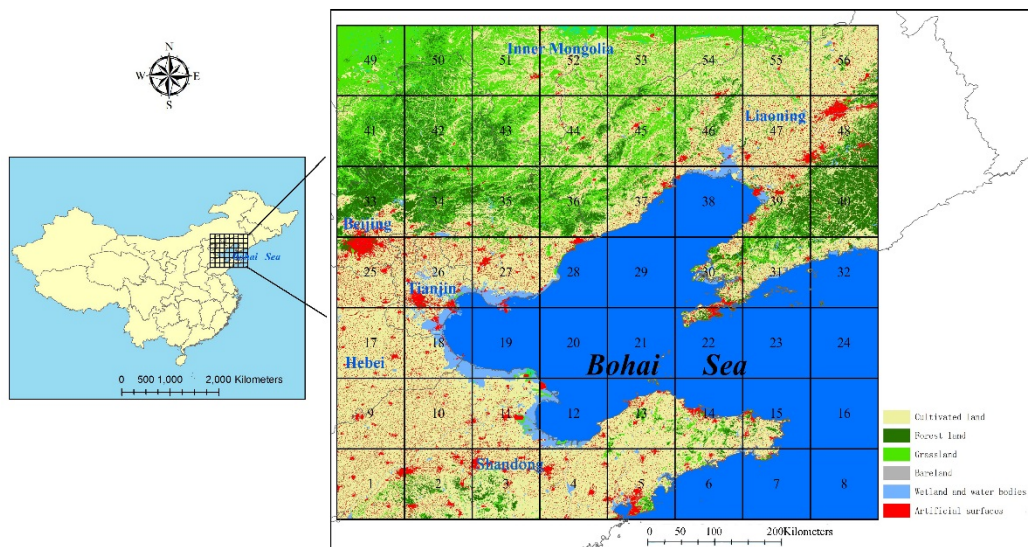
118   Fig. 2 Study area and model segmentation.

119   The longitude of Bohai Rim is from 116°E to 124°E, and the latitude is from 36°N to 43°N.

120 It is divided into 56 grids by 1°×1° (Fig. 2). For the study area, each grid contained 8

121 compartments which are lower rural air, lower urban air, rural soil, urban soil, fresh water, fresh

122 water sediment, coastal water, and vegetation. The effects of upper air were ignored as the

123 influence of long-range air transport within this region was considered to be limited. The 56

124 sub-grids are linked by advection of air, fresh water and coastal water between adjacent segments,

125 and the runoff of fresh water to coastal water was also considered.

126 2.2 Physico-chemical properties of PFOS

127   PFOS, as one of the most abundant old-generation members of PFAS family, is a kind of

128 emerging POPs, and is one of the pollutants that are most difficult to degrade. PFOS and related

129 substances are synthesized chemicals manufactured for their desirable properties of chemical

130 stability, high surface activity, and water and oil repellence (Giesy and Kannan, 2001, 2002).

131 China began to produce PFOS-based products at a large scale in 2004, and the annual production

132 of PFOS-related chemicals grew rapidly from 2003 to 2011 (Xie et al., 2013a). The

133 physical-chemical properties of PFOS included in the BETR model are listed in Table 1 (Liu,

134 2014). Additionally, in view of both hydrophobic and hydrophilic properties of PFOS (Brooke et

135 al., 2004), improvements were made to the calculation of PFOS partition coefficient duo to the

136 influence of water salinity on the sorption behavior. Full details are available in the study by (Liu

137 et al., 2015).

138   Table 1 Physico- chemical properties of PFOS

Properties	MW	M.P.	Solub	V.P.	$\mathrm{Log}(K_{OW})$	$\mathrm{Log}(K_{OA})$	$\tau_{1/2}\,\mathrm{LA}$
PFOS	538.54	400.00	519.00	3.31E-04	4.88	11.73	265500
Properties	$\tau_{1/2}$ Soil	$\tau_{1/2}$ Veg.	$\tau_{1/2}$ FW.	$\tau_{1/2}$ CW.	$\tau_{1/2}$ Sed.	E.P.	E.S.
PFOS	100000000	265500	5500000	5500000	17000000	50000	-20000

139 Notes: molar mass (MW, g/mol), melting point (M.P.,), aqueous solubility (Solub, g/m^3), vapor

140 pressure (V.P., Pa), lower air reaction half-life ($\tau_{1/2}$ LA, h), soil reaction half-life ($\tau_{1/2}$ Soil, h),

141 vegetation reaction half-life ($\tau_{1/2}$ Veg., h), fresh water reaction half-life ($\tau_{1/2}$ FW., h), coastal water

142   reaction half-life ($\tau_{1/2}$ CW., h), sediment reaction half-life ($\tau_{1/2}$ Sed., h), enthalpy of vaporization

143   from water to air (E.P., J/mol) and enthalpy of solution from octanol to water (E.S., J/mol).

144   2.3 Emission scenarios

145   According to the methodology and emission inventory developed by our research group (Xie

146   et al., 2013a;   Xie et al., 2013b), spatially distributed emissions of PFOS and its related

147   substances were estimated for the study area in 2010, which was under the hypothesis that all

148   PFOS related substances immediately degraded to PFOS (Liu et al., 2015). In this study, four

149   different future emission scenarios were proposed for the three 20-year periods to the year 2100.

150   The emission scenario 1 is called "business-as-usual (BAU)" scenario, under the assumption that

151   annual PFOS emission continues in the future till 2100. Since PFOS and its related substances

152   were listed in Stockholm Convention on POPs in 2009, the production of PFOS-related chemicals

153   fluctuated and stabilized at around 250 t/a in China from 2009 (Xie et al., 2013b). So the PFOS

154   emission till 2100 was assumed to be the same as in 2010. This is also a reference scenario in

155   order to explore the effects of climate change. Under this assumption, the emissions to each

156   compartment including fresh water, urban soil, rural soil, urban air, and rural air kept constant.

157   The reason for this assumption is that, it is easier to manage and implement the pollution control

158   measures in urban areas even if the population and land-use area of urban areas would increase till

159   2100. For rural areas, even though the population and land-use area would decrease by time (more

160   details are referred to Section 2.4), along with the shift of industrial development from urban to

161   rural areas and the improvement of people's living standard, the industrial and domestic emissions

162   would almost continue.

163   The emission scenarios 2, 3, and 4 are on the hypothesis that China would begin to phase

164   out PFOS and similar chemicals, and use alternatives fully by 2030, 2050, and 2100, respectively,

165   in compliance with the international treaties and national regulations. It is assumed that the PFOS

166   emission would linearly decrease to zero from 2016 until the year of withdrawal. Since the

167   Chinese government set a series of regulations on the production and use of PFOS in 2014 to

168   abide to the Stockholm Convention, thus encouraging the development of alternatives, while it did

169   not determine the withdrawal year, we set the above three scenarios in this study. After the

170   withdrawal year, releases will not be suddenly stopped because of applications by secondary users.

171   For all secondary users (metal plating, firefighting, textile, semiconductor, and domestic users), a

172   worst-case situation is given in which the storage of each one was within its shelf life and all

173   expired products would be treated on time. Hence, emissions from storage of secondary products

174   would continue being released during shelf-life period. Remarkably, there are some differences

175   between industrial sectors and domestic users in the future emission. For industrial sectors, taking

176   fire-fighting sector as an example, the shelf life of products is 5 years, then the releases would be

177   as the same as the previous for 5 years. For domestic applications, releases would be assumed to

178   reduce linearly as products come to the end of their natural life. For example, carpets are in use for

179   an average of about 10 years, releasing one tenth of their treatment each year until eventual

180   disposal (Paul et al., 2008). In addition, PFOS-polymers released from textile processes would

181   degrade after 30 years, because the half-life of PFOS-polymers is longer and even more than 30

182   years, and the transforming factor was 0.3 (Brooke et al., 2004). Finally, the future simulations of

183   the three 20-year periods were under the annual mean emission of each period. The estimated total

184   emissions of PFOS and their compartment distributions for the four scenarios are listed in Table

185   S1.

186   2.4 Brief introduction to climate change and urbanization scenarios

187   The following changes were implemented for each climate change scenario (Special Report

188   on Emission Scenarios (SRES) B1, A1B, and A2 in IPCC 2007): precipitation, temperature,

189   sea-level rise, soil carbon stock, and wind speed. The SRES scenarios explore alternative

190   development pathways, covering a wide range of demographic, economic and technological

191   driving forces and resulting greenhouse gas emissions. B1 describes a convergent world, a global

192   population that peaks in mid-century, but with more rapid changes in economic structures toward

193   a service and information economy. The A1B assumes a world of very rapid economic growth, a

194   global population that peaks in mid-century and rapid introduction of new and more efficient

195   technologies but a balance across all sources. A2 describes a very heterogeneous world with high

196   population growth, slow economic development and slow technological changes. The global

197   average best estimate temperature changes at 2090-2099 relative to 1980-1999 were 1.8 , 2.8 ,

198 3.4   for those three scenarios, respectively. More introductions about SRES B1, A1B, and A2

199 could be found in IPCC Climate Change 2007 Synthesis Report (IPCC, 2007). In this paper, the

200 climate change scenarios were referred to some literatures focused on China of which the results

201 were based on IPCC 2007. More details are as follows.

202   ● Precipitation

203 Gridded 10-year averaged precipitation rates in the study area were extracted from (Zhang et

204 al., 2012) for the periods 2016-2035, 2046-2065, and 2081-2100 (short of 2035, 2065, 2100 the

205 following, also called early, mid, and late 21st century respectively). Precipitation was projected to

206 increase over the study area by 3%-9% (10 yr)$^{-1}$, 7.5%-18% (10 yr)$^{-1}$, and 9%-18% (10 yr)$^{-1}$

207 respectively, under all three scenarios for the three periods.

208   ● Temperature

209 The same process was repeated for surface air temperature (Zhang et al., 2012). The warming

210 rate was projected to increase over the study area by 0.2-0.6 (10 yr)-1, 0.3-0.6 (10 yr)-1, and

211 0.1-0.6 (10 yr)$^{-1}$ respectively, under all three scenarios for the three periods. Additionally, the

212 significant feature of urbanization is "urban heat island effect", and the temperature difference

213 between urban and rural area was 2-6 (Martine and Marshall, 2007). Hence, this effect was

214 taken into account in the BETR-UR model, and it was assumed to be 4 for that difference.

215   ● Sea-level rise

216 The mean rate of averaged sea-level rise in China was 3.0 mm yr^{-1} between 1980 and 2014. It

217 was inferred that the sea-level of Bohai Sea in the early 21st century was 0.045 m higher than that

218 in 2010 for all three scenarios (China Sea Level communique 2014). The sea-level rise in mid and

219 late 21st century was referred to the global mean data in IPCC AR5, being 0.26 m, 0.25 m, 0.30 m

220 and 0.47 m, 0.48 m, 0.63 m higher under three scenarios, respectively (IPCC, 2014).

221   ● Soil carbon stock

222 The simulated averaged soil carbon stock increased by 5% for 2030s, and by 3% for 2090s

223 under scenarios B1 and A2 for northeastern China (Peng et al., 2009). Hence, it is assumed that it

224 increased by 4% for the 2060's under those two scenarios. Furthermore, since scenario A1B is a

225 moderate one between B1 and A2, we supposed that projected averaged soil C stock had the same

226 growth with those two scenarios. Additionally, a study showed that soil carbon stock was about

227 57.76% lower in urban land than that in non-construction land (forest land and green open spaces)

228   (Tao et al., 2015), which was taken into consideration in the model.

229   ● Wind speed change

230   A study using all climate model predicted that the annual mean wind speeds in China for the

231   21st century varied slightly under all three scenarios (Jiang et al., 2010). It was projected that mean

232   wind speed increased 0-1 m/s under the three scenarios for the early, mid and late 21st century in

233   the northern part of Northeastern China, middle reaches of the Yellow River and southwest of

234   Tibetan Autonomous Region. Moreover, it increased a little more under scenario A2 than the other

235   two scenarios, and it also increased more in the mid and late 21st century than the early 21st

236   century (Jiang et al., 2010). In this paper, we considered that it had a similar change pattern in the

237   Bohai Rim and northern part of Northeastern China, middle reaches of the Yellow River.

238   Besides, rainfall-runoff relationship and urbanization rate projections were analyzed. The

239   former was referred to the regression model relating mean annual runoff to mean annual

240   precipitation and mean annual temperature by (Chen and Wang, 2004). Rapid urbanization is one

241   of the outstanding features in China, particularly in coastal regions, and China is now at the peak

242   of its urban transition, where rural-urban migration has been a much more important contributor to

243   the growth (Martine and Marshall, 2007). Urban form and function also help define the nature of

244   the interactions between cities and local climate change. For example, the "urban heat island effect"

245   resulting from the impacts of different land uses in urban areas, creates microclimates and health

246   consequences. The size of the urban center, the type of urbanization, urban form, function and

247   land use all contribute to the effect. As villages grow into towns and then into cities, their average

248   temperature increases from 2 to 6 °C above that of the surrounding rural areas (Martine and

249   Marshall, 2007). Since the percentile urbanization trend of Asia from 2000 to 2050 was almost

250   consistent with the curve of urban percentage of Europe from 1950 to 2000, we therefore, assumed

251   that the rate of urbanization of China from 2051 to 2100 was likely the same as that of Europe

252   from 2000 to 2050 (Das Gupta et al., 2014).

253   3.   Results and discussion

254   3.1 Model output and validation

255   The simulations were run 18 times on steady state solutions, under each climate change

256   scenario for each emission scenario. The previous research showed that soil, coastal water, fresh

257   water, and sediment were the top four sinks for PFOS, and the storage in air and vegetation was

258   less than 1.00 %. Consequently, the concentrations and transfer process in urban soil, rural soil,

259   coastal water, fresh water, and sediment were mainly analyzed in the results of this study. The

260   median values of modeled PFOS concentrations in 2010 in fresh water, sediment, urban soil, and

261   rural soil were 8.27 ng/L, 0.38 ng/g, 0.26 ng/g, and 0.11 ng/g, respectively. Additionally, model

262   accuracy was assessed by comparing simulated baseline PFOS concentrations with measured data

263   in fresh water, fresh water sediment, urban soil, and rural soil in the study area (Table S1).

264   Available measured data for PFOS concentrations around the year 2010 were collected from

265   published sources, mostly by our research group (Li et al., 2011; Meng et al., 2015; Wang et al.,

266   2014; Wang et al., 2015; Yang et al., 2011; Zhao et al., 2014; Zhao et al., 2013; Zhu et al., 2014).

267   The results showed that the range of simulated concentrations were generally well consistent with

268   the measured data for all the compartments.

269   3.2 Spatially projected concentration changes of PFOS

270   3.2.1 Projected concentration changes of PFOS under emission scenario 1
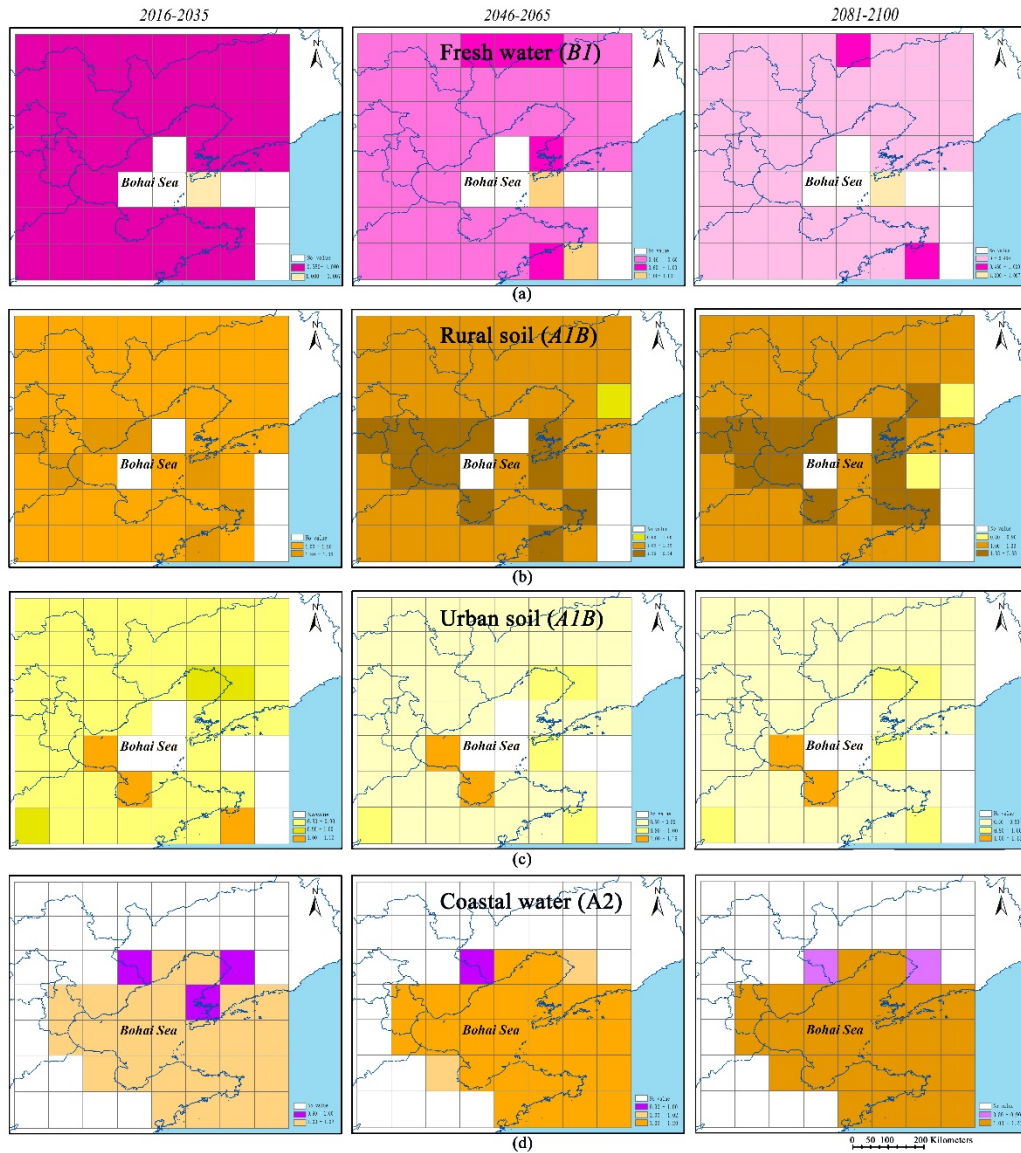
Fig. 3 Projected changes of PFOS concentrations in fresh water, rural soil, urban soil and

coastal water under specific climate change scenario for emission scenario 1.

Ratio of projected period concentration and baseline concentration was used to describe the

change of PFOS concentration in this study.

Concentration changes of PFOS for fresh water, coastal water, urban soil, and rural soil under

three future climate change scenarios and four emission scenarios were listed in Table S3. It

showed that there were similar changing trend for those four compartments among three climate

change scenarios B1, A1B and A2 under each specific emission scenario. Fig. 3 showed the

projected changes of PFOS concentrations in those four compartments under specific climate

change scenario for emission scenario 1. It could be seen that a remarkable decrease in PFOS

283 concentration in the future simulations was observed in fresh water and urban soil (except for

284 some grids). Taking grid 26 (Haihe River in Tianjin City) as an example, the concentration ratios

285 in the early, mid, and late 21st century for fresh water were 0.9616, 0.5394, 0.2772, and for urban

286 soil were 0.8708, 0.7530, 0.7533 under climate change scenario B1. And under scenarios A1B and

287 A2, fresh water concentration ratios were 0.9414, 0.4849, 0.2529 and 0.9750, 0.5203, 0.3179 in

288 the future three periods, the urban soil concentration ratios were 0.8698, 0.7515, 0.7546 and

289 0.8693, 0.7504, 0.7537 in the future three periods, respectively. Fresh water was observed with the

290 most rapid decline. The key reason for that was the increased runoff with increasing precipitation

291 even though it brought the PFOS in air to aquatic and terrestrial ecosystems through wet

292 deposition and rain dissolution with the increasing precipitation. According to the regression

293 relationship between runoff and precipitation, temperature (Chen and Wang, 2004), the runoff

294 increased a lot, particularly for the mid, and late 21st century, with a value by 5%, 25%, 32% in the

295 future three periods, respectively, under scenario B1. On the other hand, warming water would

296 reduce the solubility of PFOS (Zhou and Ma, 2013). For the urban soil, it might be because the

297 industrial and domestic emissions kept constant under the assumption of industrial shift from

298 urban to rural areas and managed domestic consumptions while with the higher urbanization rate

299 and extended urban land. On the other hand, concentrations of PFOS would decline driven by

300 temperature increasing volatilization and microbial decomposition rate. And this volatilization

301 effect driven by temperature was more significant in urban areas than rural areas because of the

302 urban heat island effect.

303   On the contrary, for most grids, the concentrations of PFOS in rural soil and coastal water

304 had the opposite trends. Taking grid 26 (Tianjin City) as an example, for rural soil, the

305 concentration ratios were 1.1705, 1.3855, 1.4618 in the future three periods under scenario A1B,

306 and the ratios for coastal water were 1.0029, 1.1688, 1.2259 under scenario A2 in the future three

307 periods, respectively. For coastal water, the runoffs from fresh water to coastal water increased

308 greatly owing to the higher temperature and precipitation, with a value of 14%, 32%, and 38% in

309 the future three periods, respectively. This would bring out the accumulation of PFOS in coastal

310 water. It was consistent with that coastal water was the final sink for PFOS (Liu et al., 2015). For

311 rural soil, under the BAU emission assumption that the related domestic consumptions increased

312 and industries clustered in rural areas while the population and land-use areas decreased in section

313   2.3, it was reasonable to show a higher concentration in the future.

314   3.2.2 Projected concentration changes of PFOS under emission reduction scenarios

315   Fig. S1- S3 showed the projected changes of PFOS concentrations in fresh water, rural soil,

316   urban soil and coastal water under specific climate change scenario for emission scenarios 2, 3 and

317   4. For emission scenario 2, the PFOS concentrations in fresh water in the whole area will decreas

318   65% or above in the early 21st century. However, in the mid 21st century, there will be some

319   growth in the southern Bohai Rim comparing to the early 21st century, and for a small number of

320   grids, the PFOS concentrations are higher than 2010. This was closely related to the emission of

321   PFOS. Because in the mid 21st century, the PFOS emission will only be from textile sector, and

322   which in the grids of southern Bohai Rim is higher than the early 21st century under the

323   assumption of emission scenario 2. For rural soil and urban soil, the PFOS concentrations will

324   decrease in the early 21st century, and decrease more in the mid 21st century except for a tiny

325   number of grids. And coastal water is the final sink of PFOS, for a big number of grids, the

326   concentrations are higher than the early 21st century, even for 2010. The trends of other three

327   compartments are almost consistent with the fresh water, because fresh water is the only medium

328   of PFOS released into the environment in the mid 21st century (Fig. S1 and Table S3).

329   For emission scenarios 3 and 4, the PFOS concentrations in the four compartments will

330   reduce with the linear emission reduction over time except for a few grids. Particularly for

331   emission scenario 3, with the PFOS withdrawn in 2050, the PFOS concentrations will decrease a

332   lot in the late 21st century, by 10 to 10,000-fold (Fig. S2, S3 and Table S3).

333   3.3 Annual mass flux changes of PFOS in Bohai Sea

334   In order to explore the impacts of climate change on the fluxes of PFOS to the Bohai Sea,

335   total annual mass flux changes were discussed under emission scenario 1 and climate change

336   scenario A1B because it was a moderate choice.

337
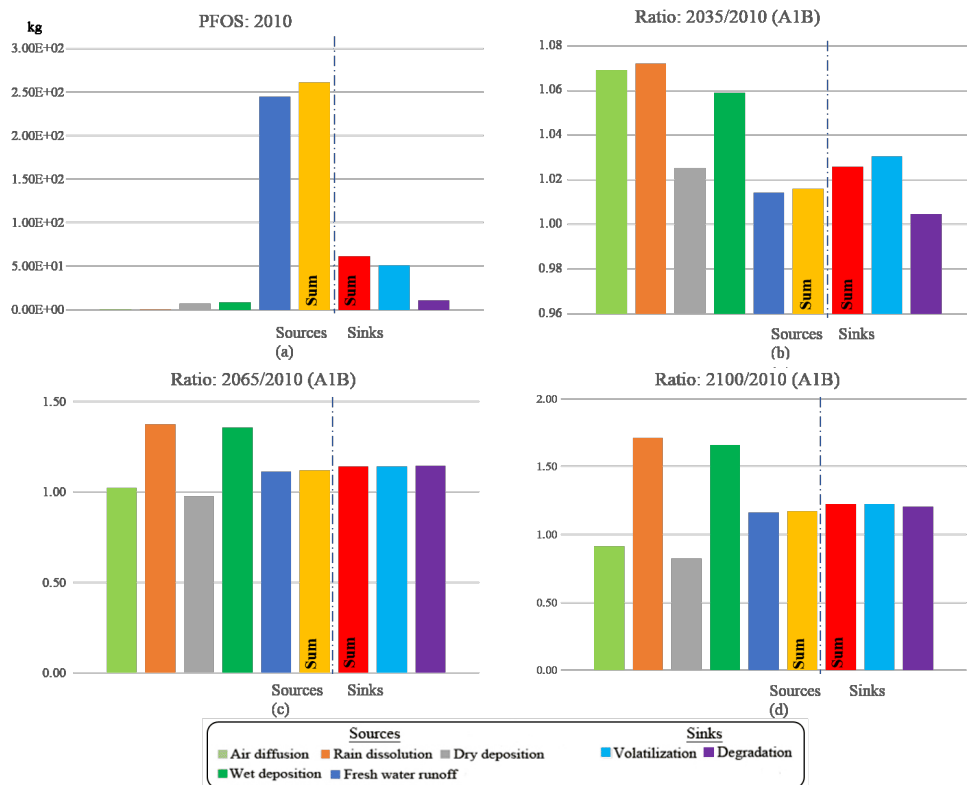
Fig. 4 Total annual mass fluxes (kg), to the Bohai Sea, sources and sinks for (a) 2010. Ratios of total annual mass fluxes: (b) 2035/2010, (c) 2065/2010, and (d) 2100/2010 under scenario A1B.

Total annual mass fluxes of PFOS to the Bohai Sea for baseline 2010, and the ratios of the fluxes for the years 2035/2010, 2065/2010 and 2100/2010 were presented in Fig. 4.

For pathways of PFOS to the Bohai Sea, rain dissolution, wet deposition, and fresh water runoff all will increase somehow in the three future periods, relative to the baseline 2010. Rain dissolution will be up by 7.21%, 37.39%, 71.00%, wet deposition will increase in ascending order by 5.91%, 35.62%, 65.94%, while fresh water runoff will increase by 1.42%, 11.39, 16.30% in 2035, 2065, and 2100, respectively, relative to 2010. These changes are due to increased precipitation in the future. Air diffusion and dry gas deposition firstly increase a little in 2035, then decrease more in 2065 and 2100, remains lower than volatilization and degradation. For sink pathways, volatilization and degradation fluxes both will increase more in the future, relative to the present (2010). This is because of the increased air and water temperature and wind speed. Total sum of sources will increase by 1.61%, 11.80%, 17.04%, and that of sinks by 2.59%, 14.30%, 22.24% in 2035, 2065, and 2100, respectively. However, the sum of sinks in 2010 was

355 much lower than the sum of sources to the Bohai Sea, so the sum of the sources (left side of the

356 dotted line) is always more than the sum of the sinks (right side of the dotted line), and the

357 differences between the sum of the sources and the sum of the sinks will be larger in the future.

358 This added to the evidence that PFOS concentrations in coastal water would increase more in the

359 future periods. It was inconsistent with the modeled results of γ-HCH and PCB 153 in the North

360 Sea (O'Driscoll et al., 2014). So the general result was that there were big influences of climate

361 change on the mass fluxes of PFOS to the Bohai Sea.

362 3.4 The changes of PFOS fate and transportation: taking Tianjin city as a case
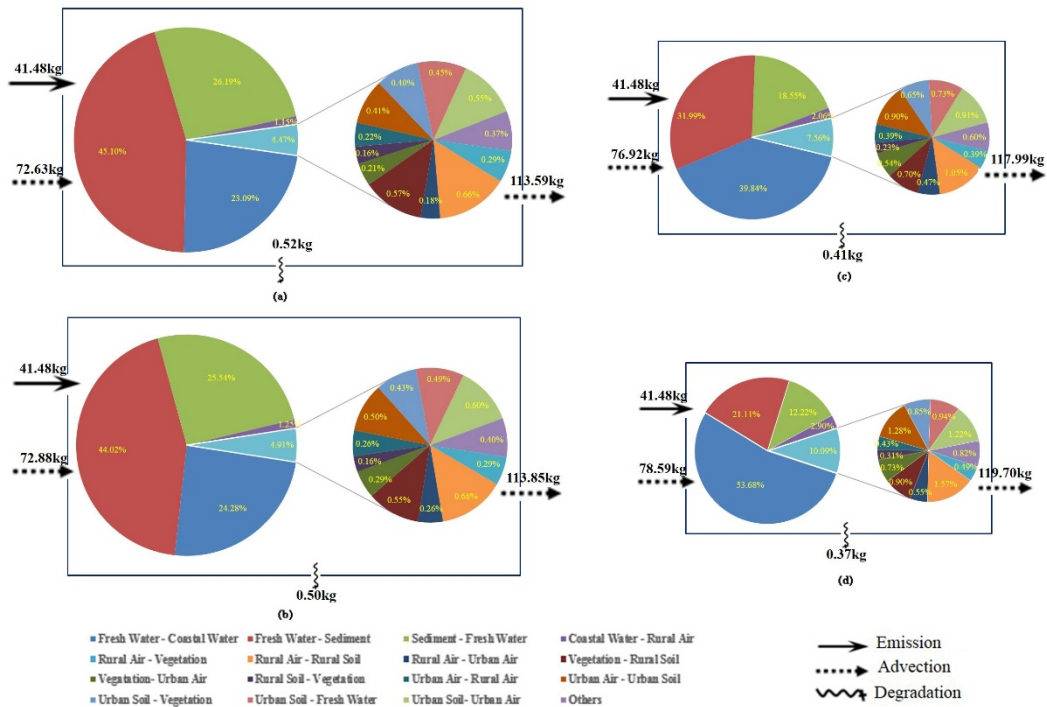
363

364   Fig. 5 The changes of PFOS fate and transportation of grid 26 under emission scenario 1 and

365   moderate climate change scenario A1B : (a) baseline 2010; (b) 2016-2035; (c) 2046-2065; (d)

366   2081-2100.

367   In this part, we took grid 26 (containing the vast majority of Tianjin City) as an example to

368 analyze the impacts of future climate change (scenario A1B) on the fate and transportation of

369 PFOS in detail, including advection fluxes between adjacent grid (inflow/outflow fluxes of air),

370 degradation rate, and intermedia transportation processes (Fig. 5). Under emission scenario 1, due

371 to the increasing mean wind speed, both the inflow and outflow fluxes will increase, particularly

372 in the mid and late 21st century, by 5.91%, 8.21% for inflow flux, and 3.87%, 5.38% for outflow

373 flux. For the not temperature dependent degradation rate, it will decline slightly with time.

374 Because the degradation rate is a complex parameter, relating to the volume of each environmental

375 compartment, PFOS concentration in each compartment, and the first-order reaction rate constant

376 (Mackay, 2001; MacLeod et al., 2001). The value in Fig. 5 was the sum of all environmental

377 compartments, hence, its reduction was maybe closely linked with the decrease of PFOS

378 concentration in fresh water, fresh water sediment, urban soil, volume of rural soil, and rural air.

379 For the intermedia transportation processes, we could see that from fresh water to coastal

380 water, fresh water to sediment, sediment to fresh water, and coastal water to rural air were the four

381 predominant transfer ways among all transfer processes (Fig. 5). Among these four pathways, the

382 transfer rate of fresh water to coastal water, coastal water to rural air increases over time,

383 particularly for the former, from 1/4 of the total in 2010 to more than half in the late 21st century.

384 It is because of increased runoffs from fresh water to coastal water led by more and more

385 precipitation in the mid and later 21st century. For the transfer rate of coastal water to rural air, it is

386 driven by temperature increasing volatilization. The transfer rate of the other two predominant

387 pathways will reduce much in the future, especially in the mid and late 21st century, decreasing by

388 5.62% - 74.55% for fresh water to sediment, and 5.73% - 74.62% for sediment to fresh water, in

389 the future (Fig. 5). According to the transfer principle between fresh water and sediment, along

390 with the concentration reduction in fresh water, the concentration in sediment will also decrease,

391 as well as the transfer rate between them.

392 4. Conclusion

393 This paper explored the potential integrative effects of future climate change and emission

394 rate on the fate and transportation of PFOS in the Bohai Rim of China using BETR-UR model,

395 taking the effects of urbanization into consideration at the same time. Our results suggested that

396 wind speed, degradation rate, and intermedia transfer processes　affect PFOS advection processes.

397 Under the influences of climate change (including temperature, precipitation, wind speed,

398 sea-level rise, and soil carbon stock) and urbanization, the projected concentrations of fresh water

399 and urban soil would decrease a lot in the future, potentially lowering the exposure burden of biota

in fresh water and urban soil. These reductions were predicted to result from increased temperature, precipitation, and urbanization. While that of coastal water and rural soil displayed an opposite trend, which would bring out more adverse effects and risk on organisms, particularly for marine ecosystem. Besides, there were big influences of climate change on the mass fluxes of PFOS to the Bohai Sea. It is important to point out that these predicted changes would occur under BAU emission. However, through modern, effective chemical management practices and legislation, chemicals with PFOS-like properties might be effectively regulated and reduced, and then concentrations of PFOS in each compartment would sharply decline and lower the risk on ecosystems. It suggests that in the future emission reduction policy-making process, climate change mitigation and adaptation should be taken into serious consideration, as well as urbanization planning.

Acknowledgement

References

China Sea Level communique 2014. China Sea Level communique. China Oceanic Administration.

Brooke, D., Footitt, A., Nwaogu, T., 2004. Environmental risk evaluation report: Perfluorooctanesulphonate (PFOS). Environment Agency Wallingford.

Chen, L., Wang, H., 2004. Sensitivity of Runoff to Climate Change in Small Drainage Basins in China. Resources Science 26, 62-68.

Das Gupta, M., Engelman, R., Levy, J., Gretchen, L., Merrick, T., Rosen, J.E., 2014. The Power

426   of the 1.8 billion, ADOLESCENTS, YOUTH AND THE TRANSFORMATION OF THE

427   FUTURE, State of world population, 2014. UNFPA, https://www. unfpa.

428   org/sites/default/files/pub-pdf/SWOP.

429   Giesy, J.P., Kannan, K., 2001. Global distribution of perfluorooctane sulfonate in wildlife.

430   Environmental science & technology 35, 1339-1342.

431   Giesy, J.P., Kannan, K., 2002. Peer reviewed: perfluorochemical surfactants in the environment.

432   Environmental science & technology 36, 146A-152A.

433   Gouin, T., Armitage, J.M., Cousins, I.T., Muir, D.C., Ng, C.A., Reid, L., Tao, S., 2013. Influence

434   of global climate change on chemical fate and bioaccumulation: The role of multimedia models.

435   Environmental Toxicology and Chemistry 32, 20-31.

436   IPCC, 2007. Synthesis Report. Contribution of Working Groups I, II and III to the Fourth

437   Assessment Report of the Intergovernmental Panel on Climate Change. IPCC, Geneva,

438   Switzerland.

439   IPCC, 2014. CLIMATE CHANGE 2014 SYNTHESIS REPORT.

440   Jiang, Y., Luo, Y., Zhao, Z., 2010. Projection of Wind Speed Changes in China in the 21st

441   Century by Climate Models. Chinese Journal of Atmospheric Sciences 34, 323-336.

442   Lamon, L., von Waldow, H., MacLeod, M., Scheringer, M., Marcomini, A., Hungerbühler, K.,

443   2009. Modeling the global levels and distribution of polychlorinated biphenyls in air under a

444   climate change scenario. Environmental science & technology 43, 5818-5824.

445   Li, F., Sun, H., Hao, Z., He, N., Zhao, L., Zhang, T., Sun, T., 2011. Perfluorinated compounds in

446   Haihe River and Dagu drainage canal in Tianjin, China. Chemosphere 84, 265-271.

447   Liu, S., 2014. Simulation of Spatial Explicit Multimedia Fate of POPs in Bohai Rim. University of

448   Chinese Academy of Sciences.

449   Liu, S., Lu, Y., Xie, S., Wang, T., Jones, K.C., Sweetman, A.J., 2015. Exploring the fate, transport

450   and risk of Perfluorooctane Sulfonate (PFOS) in a coastal region of China using a multimedia

451   model. Environment international 85, 15-26.

452   Ma, J., Cao, Z., 2010. Quantifying the perturbations of persistent organic pollutants induced by

453   climate change. Environmental science & technology 44, 8567-8573.

454   Mackay, D., 2001. Multimedia environmental models: the fugacity approach. CRC press.

455   MacLeod, M., Riley, W.J., Mckone, T.E., 2005. Assessing the influence of climate variability on

456 atmospheric concentrations of polychlorinated biphenyls using a global-scale mass balance model

457 (BETR-Global). Environmental science & technology 39, 6749-6756.

458 MacLeod, M., Woodfine, D.G., Mackay, D., McKone, T., Bennett, D., Maddalena, R., 2001.

459 BETR North America: a regionally segmented multimedia contaminant fate model for North

460 America. Environmental Science and Pollution Research 8, 156-163.

461 Martine, G., Marshall, A., 2007. State of world population 2007: unleashing the potential of urban

462 growth, State of world population 2007: unleashing the potential of urban growth. UNFPA.

463 Meng, J., Wang, T., Wang, P., Zhang, Y., Li, Q., Lu, Y., Giesy, J.P., 2015. Are levels of

464 perfluoroalkyl substances in soil related to urbanization in rapidly developing coastal areas in

465 North China? Environmental Pollution 199, 102-109.

466 O'Driscoll, K., Mayer, B., Su, J., Mathis, M., 2014. The effects of global climate change on the

467 cycling and processes of persistent organic pollutants (POPs) in the North Sea. Ocean Sci 10, 397.

468 Paul, A.G., Hammen, V.C., Hickler, T., Karlson, U.G., Jones, K.C., Sweetman, A.J., 2012.

469 Potential implications of future climate and land cover changes for the fate and distribution of

470 persistent organic pollutants in Europe. Global Ecology and Biogeography 21, 64-74.

471 Paul, A.G., Jones, K.C., Sweetman, A.J., 2008. A first global production, emission, and

472 environmental inventory for perfluorooctane sulfonate. Environmental Science & Technology 43,

473 386-392.

474 Peng, C., Zhou, X., Zhao, S., Wang, X., Zhu, B., Piao, S., Fang, J., 2009. Quantifying the response

475 of forest carbon balance to future climate change in Northeastern China: model validation and

476 prediction. Global and Planetary Change 66, 179-194.

477 Prevedouros, K., Jones, K., Sweetman, A., 2004a. European-scale modeling of concentrations and

478 distribution of polybrominated diphenyl ethers in the pentabromodiphenyl ether product.

479 Environmental science & technology 38, 5993-6001.

480 Prevedouros, K., MacLeod, M., Jones, K.C., Sweetman, A.J., 2004b. Modelling the fate of

481 persistent organic pollutants in Europe: parameterisation of a gridded distribution model.

482 Environmental Pollution 128, 251-261.

483 Song, S., Su, C., Lu, Y., Wang, T., Zhang, Y., Liu, S., 2016. Urban and rural transport of

484 semivolatile organic compounds at regional scale: A multimedia model approach. Journal of

485 Environmental Sciences 39, 228-241.

486   Tao, Y., Li, F., Wang, R., Zhao, D., 2015. Effects of land use and cover change on terrestrial

487   carbon stocks in urbanized areas: a study from Changzhou, China. Journal of Cleaner Production

488   103, 651-657.

489   Teran, T., Lamon, L., Marcomini, A., 2012. Climate change effects on POPs' environmental

490   behaviour: a scientific perspective for future regulatory actions. Atmospheric Pollution Research 3,

491   466-476.

492   Wang, P., Lu, Y., Wang, T., Fu, Y., Zhu, Z., Liu, S., Xie, S., Xiao, Y., Giesy, J.P., 2014.

493   Occurrence and transport of 17 perfluoroalkyl acids in 12 coastal rivers in south Bohai coastal

494   region of China with concentrated fluoropolymer facilities. Environmental pollution 190, 115-122.

495   Wang, P., Lu, Y., Wang, T., Zhu, Z., Li, Q., Zhang, Y., Fu, Y., Xiao, Y., Giesy, J.P., 2015.

496   Transport of short-chain perfluoroalkyl acids from concentrated fluoropolymer facilities to the

497   Daling River estuary, China. Environmental Science and Pollution Research 22, 9626-9636.

498   Wang, W., Simonich, S.L.M., Xue, M., Zhao, J., Zhang, N., Wang, R., Cao, J., Tao, S., 2010.

499   Concentrations, sources and spatial distribution of polycyclic aromatic hydrocarbons in soils from

500   Beijing, Tianjin and surrounding areas, North China. Environmental Pollution 158, 1245-1251.

501   Woehrnschimmel, H., MacLeod, M., Hungerbuhler, K., 2013. Emissions, Fate and Transport of

502   Persistent Organic Pollutants to the Arctic in a Changing Global Climate. Environmental Science

503   & Technology 47, 2323-2330.

504   Woodfine, D.G., MacLeod, M., Mackay, D., Brimacombe, J.R., 2001. Development of continental

505   scale multimedia contaminant fate models: integrating GIS. Environmental Science and Pollution

506   Research 8, 164-172.

507   Xie, S., Lu, Y., Wang, T., Liu, S., Jones, K., Sweetman, A., 2013a. Estimation of PFOS emission

508   from domestic sources in the eastern coastal region of China. Environment international 59,

509   336-343.

510   Xie, S., Wang, T., Liu, S., Jones, K.C., Sweetman, A.J., Lu, Y., 2013b. Industrial source

511   identification and emission estimation of perfluorooctane sulfonate in China. Environment

512   international 52, 1-8.

513   Yang, L., Zhu, L., Liu, Z., 2011. Occurrence and partition of perfluorinated compounds in water

514   and sediment from Liao River and Taihu Lake, China. Chemosphere 83, 806-814.

515   Zhang, L., Wu, T., Xin, X., Dong, M., Wang, Z., 2012. Projections of annual mean air temperature

516   and precipitation over the globe and in China during the 21st century by the BCC Climate System

517   Model BCC_CSM1. 0. Acta Meteorologica Sinica 26, 362-375.

518   Zhao, X., Xia, X., Zhang, S., Wu, Q., Wang, X., 2014. Spatial and vertical variations of

519   perfluoroalkyl substances in sediments of the Haihe River, China. Journal of Environmental

520   Sciences 26, 1557-1566.

521   Zhao, Z., Tang, J., Xie, Z., Chen, Y., Pan, X., Zhong, G., Sturm, R., Zhang, G., Ebinghaus, R.,

522   2013. Perfluoroalkyl acids (PFAAs) in riverine and coastal sediments of Laizhou Bay, North

523   China. Science of the total environment 447, 415-423.

524   Zhou, Z., Ma, L., 2013. Research advance of climate change influence on environmental behavior

525   of POPs. Environmental Pollution & Control 35, 84-87.

526   Zhu, Z., Wang, T., Wang, P., Lu, Y., Giesy, J.P., 2014. Perfluoroalkyl and polyfluoroalkyl

527   substances in sediments from South Bohai coastal watersheds, China. Marine pollution bulletin 85,

528   619-627.

529